Probing confinement through dynamical quantum phase transitions: From quantum spin models to lattice gauge theories

Jesse J. Osborne [1,*] Ian P. McCulloch [2,3,1,†] and Jad C. Halimeh [4,5,6,‡]

[1]School of Mathematics and Physics, The University of Queensland, St. Lucia QLD 4072, Australia
[2]Department of Physics, National Tsing Hua University, Hsinchu 30013, Taiwan
[3]Frontier Center for Theory and Computation, National Tsing Hua University, Hsinchu 30013, Taiwan
[4]Max Planck Institute of Quantum Optics, 85748 Garching, Germany
[5]Department of Physics and Arnold Sommerfeld Center for Theoretical Physics (ASC), Ludwig Maximilian University of Munich, 80333 Munich, Germany
[6]Munich Center for Quantum Science and Technology (MCQST), 80799 Munich, Germany

(Received 28 January 2024; accepted 24 July 2025; published 17 October 2025)

Confinement is an intriguing phenomenon prevalent in condensed matter and high-energy physics. Exploring its effect on the far-from-equilibrium criticality of quantum many-body systems is of great interest from both a fundamental and a technological point of view. Here, we employ large-scale uniform matrix product state calculations to show that a qualitative change in the type of dynamical quantum phase transitions (DQPTs) accompanies the confinement-deconfinement transition in three paradigmatic models: the power-law interacting quantum Ising chain, the two-dimensional quantum Ising model, and the spin-S U(1) quantum link model. By tuning a confining parameter in these models, it is found that *branch* (*manifold*) DQPTs arise as a signature of (de)confinement. Whereas manifold DQPTs are associated with a sign change of the order parameter, their branch counterparts are not, but rather occur even when the order parameter exhibits considerably constrained dynamics. Our conclusions can be tested in modern quantum-simulation platforms, such as ion-trap setups and cold-atom experiments of gauge theories.

DOI: 10.1103/rnv5-f32k

I. INTRODUCTION

Confinement is a prominent effect in physics, most famous in the context of color confinement in quantum chromodynamics (QCD). Below the Hagedorn temperature, color-charged particles, such as quarks and gluons, cannot be isolated and are confined into hadrons [1]. Confinement is also present in the context of another gauge theory, quantum electrodynamics (QED). There, a topological θ angle [2–4] or the gauge coupling [5] can be tuned to induce confinement. Recently, there has been significant interest in probing confinement of gauge theories on dedicated large-scale quantum simulators [6–13], including at finite temperature [14–16].

Beyond gauge theories, confinement can also arise in the context of quantum spin chains. If one considers a quantum Ising chain with transverse and longitudinal fields, then real-time confinement in the wake of a quantum quench arises, where domain-wall excitations due to the transverse field tend to bind together due to the longitudinal field [17]. Confinement also occurs in transverse-field Ising chains with long-range interactions [18–20], where the latter also makes it energetically unfavorable for domain-wall excitations to be separated at long distances. The two-dimensional (2D) Ising model also exhibits confinementlike behavior [21,22]. With nearest-neighbor interactions, the energy of a domain (or island) of opposite spin polarization in the ferromagnetic phase is proportional to the size of its boundary, which generally grows as the domain is expanded in two spatial dimensions, in contrast to the one-dimensional case, where it is constant. Dynamically, this leads to a suppression of the spread of such domains in the two-dimensional model when the transverse-field strength is not large enough.

Whether in quantum spin models or gauge theories, the presence of confinement gives rise to exotic constrained dynamics that is very interesting to understand from a fundamental point of view, and also to possibly probe on modern quantum simulators [23–31].

In recent years, there has been a concerted effort to build a complete theoretical framework of far-from-equilibrium quantum many-body criticality. Various approaches have been explored, with one particular avenue that has garnered significant attention: dynamical quantum phase transitions (DQPTs) [32–34]. It entails extending the concept of thermal free energy in equilibrium to Schrödinger time evolution. By recognizing that the overlap of the time-evolved wave function

*Contact author: j.osborne@student.uq.edu.au
†Contact author: ian@phys.nthu.edu.tw
‡Contact author: jad.halimeh@physik.lmu.de

Published by the American Physical Society under the terms of the Creative Commons Attribution 4.0 International license. Further distribution of this work must maintain attribution to the author(s) and the published article's title, journal citation, and DOI. Open access publication funded by Max Planck Society.

with the initial state is a boundary partition function, one can interpret evolution time as complexified inverse temperature. The logarithm of this overlap is then related to a *dynamical* free energy whose nonanalyticities at *critical evolution times* are DQPTs. DQPTs have been extensively studied over the last decade in nonintegrable short-range quantum spin chains [35–37], long-range models [38–48], topological systems [49–57], in higher spatial dimensions [50,58–63], at finite temperature [64–69], and in gauge theories [70–76], and they have been observed experimentally [77–79].

In this study, we ask: Can DQPTs be leveraged as a probe of confinement in quantum many-body models? Given that DQPTs offer a window into out-of-equilibrium criticality, and considering that confinement fundamentally changes the nature of the dynamics of a quantum many-body system, it would be prudent to investigate this question, which we do using state-of-the-art numerical methods. We find that the presence of confinement fundamentally changes the type of DQPTs that dominate the return rate of a quenched quantum many-body system. To demonstrate our findings, we consider three paradigmatic systems: the long-range quantum Ising chain, the two-dimensional quantum Ising model on a square lattice, and spin-S U(1) quantum link model (QLM) formulations of lattice QED.

II. LONG-RANGE QUANTUM ISING CHAIN

We consider the nonintegrable long-range transverse-field Ising chain (LR-TFIC) with power-law interactions, described by the Hamiltonian

$$\hat{H}_{\text{LR-TFIC}} = -J\sum_{j>i}\frac{1}{|j-i|^{\alpha}}\hat{\sigma}_i^z\hat{\sigma}_j^z - h\sum_i \hat{\sigma}_i^x, \tag{1}$$

where $\hat{\sigma}_i^{x,z}$ are the x and z Pauli matrices acting on site i, J is the spin coupling constant, h is the magnetic-field strength, and α is the exponent of the power law. The LR-TFIC at ferromagnetic coupling ($J > 0$) has a thermal phase transition for $\alpha < 2$, a phase transition of the Berezinskii-Kosterlitz-Thouless [80–82] type at finite temperature for $\alpha = 2$, and no thermal phase transition for $\alpha > 2$ [83]. It hosts a quantum phase transition at an α-dependent critical value of the transverse-field strength h for any α, and this transition is related to the spontaneous breaking of a global $\mathbb{Z}_2$ symmetry [84]. For $\alpha \geqslant 3$, it falls in the same short-range universality class as the nearest-neighbor model, while for $\alpha < 2$, it exhibits long-range universality, with critical exponents that vary with α [83]. In this work, we consider ferromagnetic coupling ($J > 0$) and inverse-square interactions ($\alpha = 2$), although we have checked that our following conclusions are valid for other values of α.

We initialize the system in the ground-state manifold at $h = h_{\text{i}} = 0$, which is spanned by the basis states $|\psi^+\rangle = |\cdots\uparrow\uparrow\uparrow\uparrow\uparrow\cdots\rangle$ and $|\psi^-\rangle = |\cdots\downarrow\downarrow\downarrow\downarrow\downarrow\cdots\rangle$. We choose the initial state $|\psi(t=0)\rangle = |\psi^+\rangle$ and suddenly quench the magnetic field to $h = h_{\text{f}} > 0$, obtaining the time-evolved wave function $|\psi(t)\rangle = e^{-i\hat{H}_{\text{LR-TFIC}}t}|\psi^+\rangle$ at evolution time t, where we have set the reduced Planck constant to $\hbar = 1$. To numerically simulate the time evolution of this state, we use infinite matrix product state (iMPS) techniques, which work directly in the thermodynamic limit by writing the state in a translation-invariant form [85–88]. Specifically, we use a version of the time-dependent variational principle algorithm [89,90] that has been modified to handle translation-invariant states. We use single-site evolution with adaptive bond expansion, with a time step of $0.001/J$. As the inverse-square interaction cannot be directly represented as a matrix product operator (MPO) with finite bond dimension, we instead fit a weighted sum of five exponential functions [91], which has an efficient representation as an MPO with a total error of less than 10^{-8} over the first 100 sites.

To detect the DQPTs in the time-evolution simulations, we calculate the expectation value of the order parameter, namely, the net magnetization $\mathcal{M}^z(t) = \lim_{L\to\infty}\sum_j\langle\psi(t)|\hat{\sigma}_j^z|\psi(t)\rangle/L$, which is related to the spontaneous breaking of the global $\mathbb{Z}_2$ symmetry hosted by the LR-TFIC, and we also calculate the return rates with the two degenerate ground states at $h = 0$, defined by

$$\lambda_1^{\pm}(t) = -\lim_{L\to\infty}\frac{1}{L}\ln|\langle\psi^{\pm}|\psi(t)\rangle|^2. \tag{2}$$

We define the *total* return rate as the minimum of these two values [77], $r(t) = \min\{\lambda_1^+(t), \lambda_1^-(t)\}$. These return rates have a well-defined value in the thermodynamic limit and can be calculated from the leading eigenvalue $\epsilon^{\pm}(t)$ of the mixed iMPS transfer matrix $\mathcal{T}^{\pm}(t)$ [92] between $|\psi(t)\rangle$ and $|\psi^{\pm}\rangle$, so that $\lambda^{\pm}(t) = -\ln|\epsilon^{\pm}(t)|^2$. DQPTs are defined as nonanalyticities in this total return rate $r(t)$ [33], which either correspond to *manifold crossings* between $\lambda^+(t)$ and $\lambda^-(t)$ or are so-called anomalous DQPTs where there is no manifold crossing. We can better understand these anomalous DQPTs as *branch crossings* in the full eigenvalue spectrum of the transfer operator (in order of decreasing magnitude) $\epsilon_n^{\pm}(t)$, $n = 1, 2, \ldots$ [74,85], from which we analogously define the higher-order return rates $\lambda_n^{\pm}(t) = -\ln|\epsilon_n^{\pm}(t)|^2$.

An equivalent method of calculating the return rates (2) is to calculate time-evolution simulations for each initial state $|\psi^{\pm}(t)\rangle$ and evaluate $\lambda_1^{\pm}(t) = -\lim_{L\to\infty}L^{-1}\ln|\langle\psi^{\pm}(-t/2)|\psi^+(t/2)\rangle|^2$, where we obtain $|\psi^{\pm}(-t/2)\rangle$ by taking the complex conjugate of $|\psi^{\pm}(t/2)\rangle$, as the initial state is time-reversal symmetric. By using this *doubling trick*, if we perform a time-evolution simulation up to time T for each initial state, we can calculate the return rates up to time $2T$. And since the return rates are much more susceptible to error than local observables such as the magnetization, we can perform another time-evolution simulation with a larger MPS truncation threshold, which will give converged results for the order parameter to longer times as well.

The dynamical critical point h_{c}^{d} is defined such that the infinite-time average of the order parameter is nonzero if the quenched value of the transverse-field strength h_{f} is less than h_{c}^{d}, while if $h_{\text{f}} > h_{\text{c}}^{\text{d}}$, then the infinite-time average of the order parameter is zero [93,94]. (The value of h_{c}^{d} also depends on the initial value h_{i} of the quench parameter.) For inverse-square interactions $\alpha = 2$, the dynamical critical point of the LR-TFIC when $h_{\text{i}} = 0$ is $h_{\text{c}}^{\text{d}} \approx 1.85J$ [39,40]. When we quench to a magnetic field below the dynamical critical point $h_{\text{f}} < h_{\text{c}}^{\text{d}}$, we only observe DQPTs corresponding to branch crossings, and the order parameter does not pass zero, as shown in Fig. 1(a) for $h_{\text{f}} = 1.25J$. This is indicative of constrained

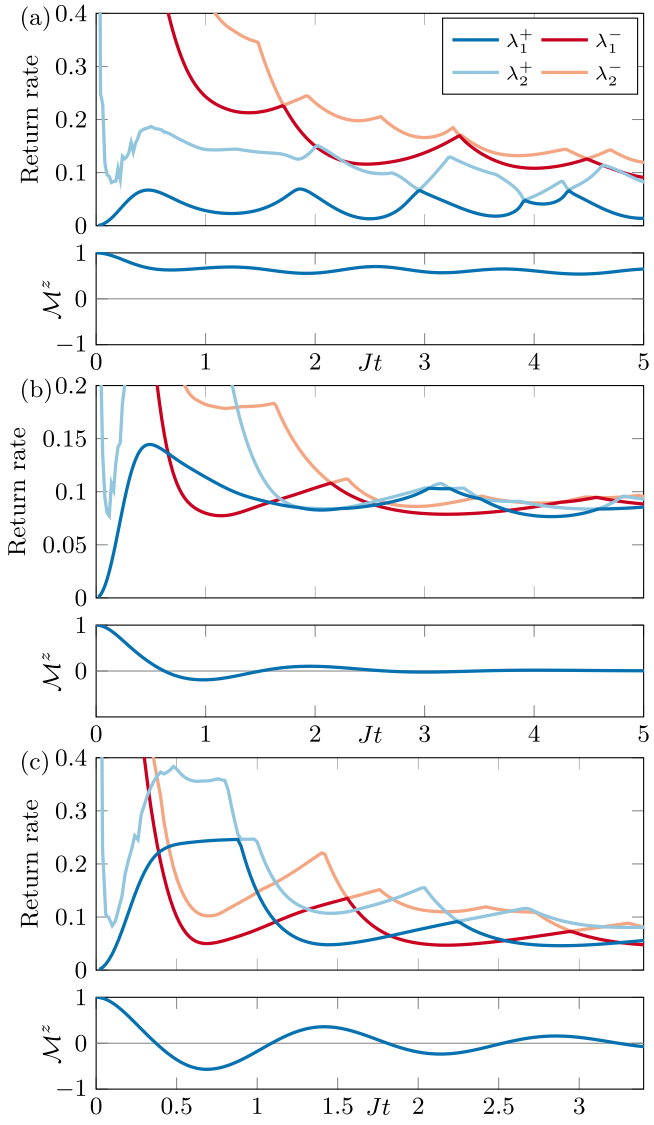


FIG. 1. The return rates and order parameter of the quench of the inverse-square long-range transverse-field Ising chain [Eq. ((1) from $h_i = 0$ to (a) $h_f = 1.25J < h_c^d$, (b) $h_c^d < h_f = 1.9J < h_{cross}$, and (c) $h_f = 2.5J > h_{cross}$. The lines with different hues correspond to return rates calculated with different initial manifold states, while lighter shades represent the higher branches (as discussed in the main text). Dynamical quantum phase transitions are indicated by the crossing of the two lowest curves, which may be different hues (i.e., from different manifolds, and this is thus a manifold DQPT), or between two shades of the same hue (i.e., the two lowest branches of the same manifold, thus a branch DQPT).

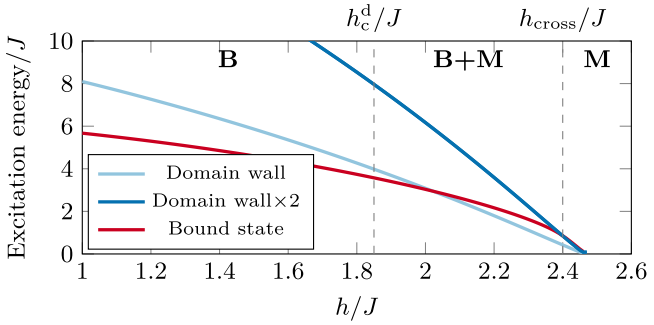


FIG. 2. The excitation energies in the inverse-square long-range transverse-field Ising chain [Eq. (1)]. We show the energies calculated using the MPS excitation ansatz for topologically nontrivial domain walls between the two ground states (showing both single and double domain-wall energies), as well as topologically trivial bound states. We show the approximate locations of the dynamical critical point h_c^d, above which we observe manifold (**M**) DQPTs, and the crossover point h_{cross}, below which there is an energy gap between the lowest bound state excitation and two isolated domain walls. The presence of branch (**B**) DQPTs is thought to be related to this crossover point h_{cross} [19].

dynamics, where the evolved state does not vary far from the initial state. However, if we quench above the dynamical critical point $h_f > h_c^d$, we observe DQPTs corresponding to manifold crossings, each of which is associated with the order parameter crossing zero, as shown in Figs. 1(b) and 1(c) for $h_f = 1.9J$ and $2.5J$, respectively.

Although the dynamical critical point h_c^d corresponds with the appearance of *manifold* DQPTs, it is not directly connected to *branch* DQPTs. Indeed, for quenches just past this critical point, we observe both branch and manifold DQPTs, as in Fig. 1(b) for $h_f = 1.9J$, while further from the critical point, we only observe manifold DQPTs within accessible times, as in Fig. 1(c) for $h_f = 2.5J$. The presence of branch DQPTs is instead related to a crossover in the behavior of the quasiparticle excitations of this model, as established in Refs. [19,95]: Below the equilibrium critical point ($h_c^e \approx 2.5J$ in this case [39]), for $h > h_{cross} \approx 2.4J$, the lowest energy excitations are noninteracting domain walls, but for $h < h_{cross}$, a bound state of two domain walls has a lower energy than two vastly separated domain walls. We plot the energies of free and bound domain-wall excitations in Fig. 2, calculated using the MPS excitation ansatz [95–97], showing the regions where branch, manifold, or both types of DQPTs occur. This highlights the relevance of the confinement-deconfinement transition between bound and freely propagating excitations to the appearance of manifold DQPTs.

III. TWO-DIMENSIONAL QUANTUM ISING MODEL

We now turn to the 2D transverse-field Ising model on a square lattice, whose Hamiltonian is

$$\hat{H}_{\text{2D-TFIM}} = -J \sum_{\langle \mathbf{i},\mathbf{j} \rangle} \hat{\sigma}_{\mathbf{i}}^z \hat{\sigma}_{\mathbf{j}}^z - h \sum_{\mathbf{i}} \hat{\sigma}_{\mathbf{i}}^x, \tag{3}$$

where $\mathbf{i}$ is a vector index marking the location of a site on the square lattice. Unlike its one-dimensional counterpart, the 2D Ising model with nearest-neighbor interactions has a finite-temperature phase transition at a critical (Onsager) temperature of $T_c = 2J/\ln(1+\sqrt{2})$ [98]. On the square lattice, it has a quantum phase transition at the equilibrium critical point $h_c^e \approx 3.004J$ [99,100].

As is standard for studying 2D systems using MPS techniques, we put the system onto a cylindrical geometry with a finite circumference of L_y sites, while the system is in the thermodynamic limit in the axial direction $L_x = \infty$. For the results of this work, we set $L_y = 6$ sites. Due to the finite length in the y direction, finite-size fluctuations reduce the

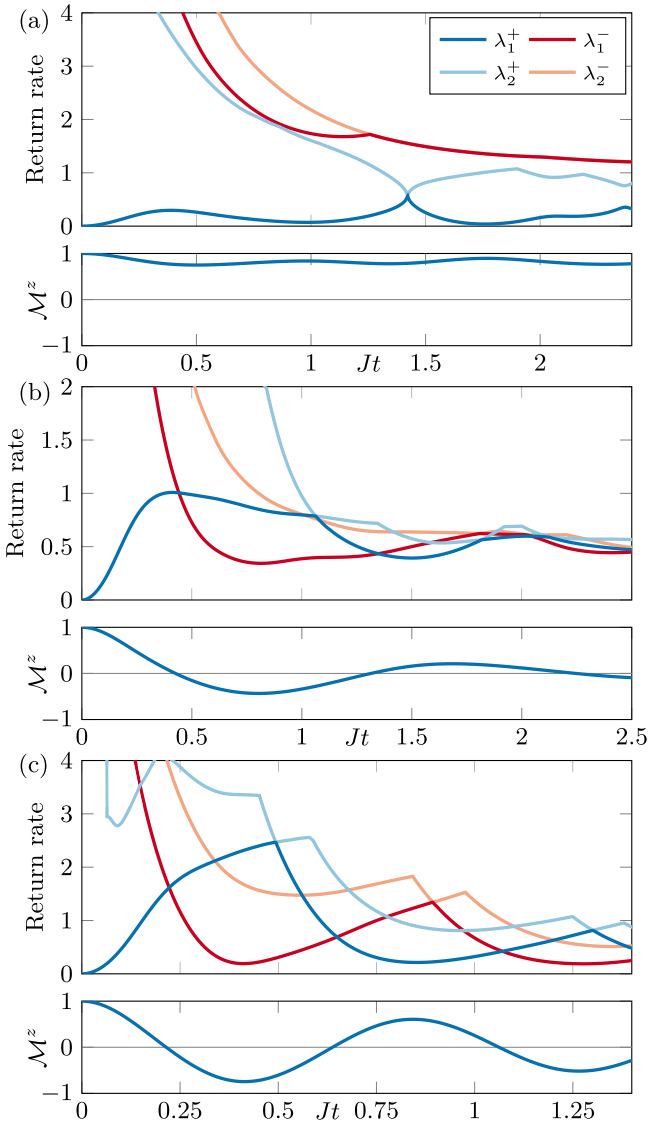


FIG. 3. The return rates and order parameter of the quench of the transverse field in the two-dimensional square-lattice transverse-field Ising model [Eq. (3)] on a cylindrical geometry with circumference $L_y = 6$, from $h_i = 0$ to (a) $h_f = 1.3J < h_c^d$, (b) $h_c^d < h_f = 2.5J < h_{cross} = h_c^e$, and (c) $h_f = 4J > h_{cross} = h_c^e$.

equilibrium quantum critical point to $h_c^e \approx 2.93J$, and based on the order-parameter dynamics, the dynamical critical point is $h_c^d \approx 2.0J$ [101]. Since domain walls have an unbounded energy in two spatial dimensions, the lowest excitation energies will be topologically trivial, and so the excitation crossover energy h_{cross} will be identical to the equilibrium critical point h_c^e. Our results are shown in Fig. 3: When we quench below the dynamical critical point [$h_f = 1.3J < h_c^d$ in Fig. 3(a)], we only observe branch DQPTs and the order parameter is significantly above zero, indicating constrained dynamics, while when we quench above the dynamical critical point $h_c^d \approx 1.85J$, we observe manifold DQPTs corresponding to zero crossings of the order parameters. Branch DQPTs still persist below the crossover point $h_{cross} = h_c^e \approx 2.93J$, as we can see in Fig. 3(b) for $h_f = 2.5J$, but disappear from the accessible evolution times above this point, as in Fig. 3(c) for $h_f = 4J$.

As such, the same picture holds as in the case of the LR-TFIC: In the presence of confinement, branch DQPTs arise and dominate the return rate concurrently with the order parameter exhibiting constrained dynamics and never passing zero, while in the deconfined phase, manifold DQPTs dominate the return rate and correspond directly to order-parameter zeros, with branch DQPTs persisting until a crossover point.

IV. SPIN-S U(1) QUANTUM LINK MODEL

Let us now consider a paradigmatic gauge theory, the spin-S U(1) quantum link model (QLM) with Hamiltonian [102–104]

$$\hat{H}_{QLM} = -\frac{\kappa}{2}\sum_i (\hat{\phi}_i^\dagger \hat{s}_{i,i+1}^+ \hat{\phi}_{i+1} + \text{H.c.}) + \mu\sum_i (-1)^i \hat{\phi}_i^\dagger \hat{\phi}_i + \frac{g^2}{2}\sum_i \left(\hat{s}_{i,i+1}^z\right)^2, \quad (4)$$

where $\hat{\phi}_i^\dagger$ ($\hat{\phi}_i$) is a fermionic creation (annihilation) operator acting on matter site i, where even (odd) sites represent (anti)particles (and for antiparticles, the role of creation and annihilation is swapped), $\hat{s}_{i,i+1}^\pm$ and $\hat{s}_{i,j+1}^z$ are spin-S operators acting on the gauge link between matter sites i and $i+1$, representing the gauge and electric-field operators, respectively, κ is the hopping energy, μ is the fermion mass, and g is the gauge-coupling strength, which controls the confinement of the particles.

The generators of the U(1) gauge symmetry are

$$\hat{G}_i = \hat{s}_{i,i+1}^z - \hat{s}_{i-1,i}^z - \hat{\phi}_i^\dagger \hat{\phi}_i - \frac{(-1)^i - 1}{2}, \quad (5)$$

which are a discrete analog of Gauss's law. We work in the physical sector where $\hat{G}_i|\psi\rangle = 0, \forall i$.

In this work, we consider $S = 1$ (the effect of the gauge coupling g is trivial for $S = 1/2$, as then $(\hat{s}_{i,i+1}^z)^2 = \mathbb{1}/4$ is an inconsequential constant energy term) where there are three different vacua in the physical sector, which can be written in a basis characterized by the z projection of the spin m_z of each link flux: $\hat{s}_{i,i+1}^z|\psi^{m_z}\rangle = m_z|\psi^{m_z}\rangle$, $\forall i$, where $m_z = -1, 0, +1$ (we will write $m_z = \pm$ as an abbreviation of ± 1 in the superscript). We then numerically simulate a sudden quench from the "extreme" vacuum $|\psi^+\rangle$ to a finite g and μ using the same numerical methods as in the previous sections with a time step of $0.01/\kappa$, and we calculate the return rates $\lambda_1^{0,\pm}(t)$ for the three vacua, with the total return rate $r(t) = \min\{\lambda_1^+(t), \lambda_1^0(t), \lambda_1^-(t)\}$ being their minimum, as well as the electric flux $\mathcal{E}(t) = \lim_{L\to\infty}\sum_i \langle\psi(t)|\hat{s}_{i,i+1}^z|\psi(t)\rangle/L$, which is an order parameter associated with a global $\mathbb{Z}_2$ symmetry related to charge-parity conservation [105,106].

The gauge coupling g tunes the strength of confinement. For small g, confinement is weak: This is shown in the behavior of the flux in our quenches to $g_f = 0$ and 0.6κ in Figs. 4(a) and 4(b). In these quenches, the flux oscillates close to the extreme values ± 1, which is indicative of the free propagation of single deconfined matter particles. We also observe primarily manifold DQPTs, with a zero crossing of the flux corresponding to a maximal overlap of the wave function with the middle vacuum. At larger values of g, such as in the quench to $g_f = 1.4\kappa$ in Fig. 4(c), confinement is strong, as

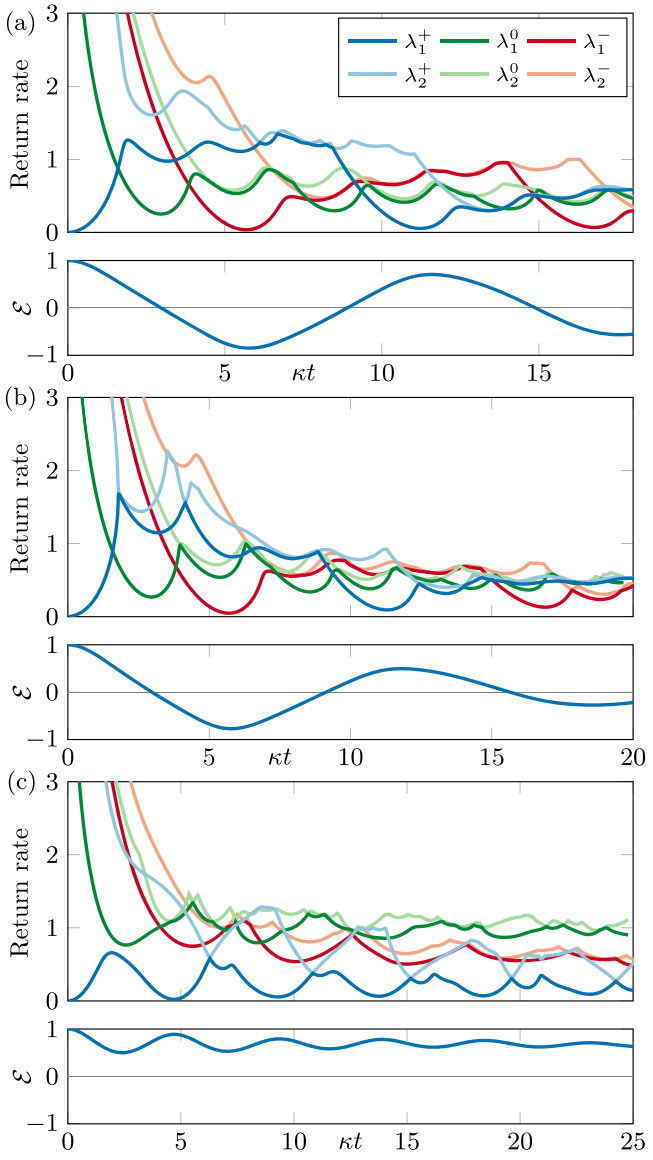


FIG. 4. The return rates and order parameter of the quench of the spin-1 U(1) QLM [Eq. (4)], $\mu = 0.1\kappa$, from the positive extreme vacuum $|\psi^+\rangle$ to (a) $g_f = 0$, (b) $g_f = 0.6\kappa$, and (c) $g_f = 1.4\kappa$.

indicated by the flux oscillating close to its initial value. In this case, we only observe branch DQPTs and no manifold DQPTs at all.

In fact, we can observe branch DQPTs in all of these quenches. This is consistent with the fact that single-particle excitations are domain walls between different vacuum flux sectors, which have different energy densities for finite m, even for $g = 0$, and so single-particle excitations will always be energetically unbounded, and the lowest-lying excitations will be two-particle bound states. Nevertheless, we can see that branch DQPTs are more abundant for larger g_f, where we expect the effect of confinement to be greater.

V. DISCUSSION AND OUTLOOK

We have shown how the prevalence of *branch* DQPTs in the return rate, which involve nonanalyticities in the overlap to the initial state, is an indicator of confinement. We have demonstrated this using iMPS calculations involving the power-law interacting quantum Ising chain, quantum Ising model on a square lattice, and spin-S U(1) QLMs of lattice QED. Our numerical simulations show a clear picture: In the deconfined phase, manifold DQPTs arise that have a direct connection to order-parameter zeros and disappear at the dynamical critical point, after which the order parameter exhibits constrained dynamics near its initial value. The appearance of branch DQPTs is unrelated to this dynamical critical point. Rather, the point of appearance of branch DQPTs coincides with a crossover in the energy of the lowest-lying excitations from bound pairs to freely propagating domain walls and is thus intimately related to confinement.

Given the high level of control and precision in today's quantum simulators, our conclusions can be tested in ion-trap and cold-atom setups [77,107]. Whereas in Ref. [77] only those regimes in which manifold DQPTs occur were probed, quenches within the ferromagnetic phase of the long-range quantum Ising chain would be able to exhibit branch DQPTs while simultaneously observing constrained order-parameter dynamics, the latter as explained in Ref. [18]. For the spin-1 U(1) QLM, recent experimental proposals have shown how this can be realized using bosonic dysprosium atoms in optical superlattices, which would facilitate the verification of our conclusions in lattice gauge theories [108].

It would be interesting to understand how confinement gives rise to branch DQPTs. Given that the models considered here are nonintegrable and their far-from-equilibrium dynamics is highly nonperturbative, analytic insights are limited, and numerical methods become our best approach to understanding the physics. Nevertheless, one can speculate that confinement gives rise to fundamentally *far-from-equilibrium* criticality in the form of branch DQPTs, distinct from the rather equilibriumlike criticality of manifold DQPTs, which are directly associated with the order-parameter dynamics changing sign. Furthermore, and unsurprisingly, it seems that the criticality of branch DQPTs involves much higher-order excitations than the low-lying quasiparticles due to confinement such as bound domain walls in the LR-TFIC, because low-energy approximations of the LR-TFIC such as the two-kink model [18] do not capture branch DQPTs.

It is worth mentioning that we have intentionally chosen models with unbroken global symmetries, in order to be able to properly define and distinguish between manifold and branch DQPTs. Of course, there are models such as the Ising chain with both transverse and longitudinal fields and the spin-1/2 U(1) QLM with a topological θ term in which the global symmetry is explicitly broken. In such a case, the initial-state manifold is nondegenerate, and the return rate involves projecting on a single initial state, thereby preventing a distinction between manifold and branch DQPTs. This is something we have intentionally avoided for clarity. With that said, classifying confinement in such models through DQPTs would also be interesting and is left for future work.

ACKNOWLEDGMENTS

J.C.H. acknowledges funding by the Max Planck Society, the Deutsche Forschungsgemeinschaft (DFG,

German Research Foundation) under Germany's Excellence Strategy—EXC-2111—Grant No. 390814868, the European Research Council (ERC) under the European Union's Horizon Europe research and innovation program (Grant Agreement No. 101165667)—ERC Starting Grant QuSiGauge, funding within the QuantERA II Programme that has received funding from the European Union's Horizon 2020 research and innovation program under Grant Agreement No 101017733, support by the QuantERA grant DYNAMITE, and funding from the European Research Council (ERC) under the European Union's Horizon 2020 research and innovation program (Grant Agreement No. 948141)—ERC Starting Grant SimUcQuam. I.P.M. acknowledges funding from the National Science and Technology Council of Taiwan (NSTC) Grants No. 112-2811-M-007-044 and No. 113-2112-M-007-MY2. Numerical simulations were performed on The University of Queensland's School of Mathematics and Physics Core Computing Facility `getafix`. This work is part of the Quantum Computing for High-Energy Physics (QC4HEP) working group.

DATA AVAILABILITY

No data were created or analyzed in this article.

[1] R. Ellis, W. Stirling, and B. Webber, *QCD and Collider Physics*, *Cambridge Monographs on Particle Physics, Nuclear Physics and Cosmology* (Cambridge University Press, Cambridge, 2003).

[2] G. 't Hooft, Computation of the quantum effects due to a four-dimensional pseudoparticle, Phys. Rev. D **14**, 3432 (1976).

[3] R. Jackiw and C. Rebbi, Vacuum periodicity in a Yang-Mills quantum theory, Phys. Rev. Lett. **37**, 172 (1976).

[4] C. G. Callan, R. F. Dashen, and D. J. Gross, Instantons as a bridge between weak and strong coupling in quantum chromodynamics, Phys. Rev. D **20**, 3279 (1979).

[5] S. Chandrasekharan, Confinement, chiral symmetry breaking and continuum limits in quantum link models, Nucl. Phys. B **73**, 739 (1999).

[6] E. Zohar, J. I. Cirac, and B. Reznik, Simulating compact quantum electrodynamics with ultracold atoms: Probing confinement and nonperturbative effects, Phys. Rev. Lett. **109**, 125302 (2012).

[7] J. Mildenberger, W. Mruczkiewicz, J. C. Halimeh, Z. Jiang, and P. Hauke, Confinement in a $\mathbb{Z}_2$ lattice gauge theory on a quantum computer, Nat. Phys. **21**, 312 (2025).

[8] J. C. Halimeh, I. P. McCulloch, B. Yang, and P. Hauke, Tuning the topological θ-angle in cold-atom quantum simulators of gauge theories, PRX Quantum **3**, 040316 (2022).

[9] Y. Cheng, S. Liu, W. Zheng, P. Zhang, and H. Zhai, Tunable confinement-deconfinement transition in an ultracold-atom quantum simulator, PRX Quantum **3**, 040317 (2022).

[10] W.-Y. Zhang, Y. Liu, Y. Cheng, M.-G. He, H.-Y. Wang, T.-Y. Wang, Z.-H. Zhu, G.-X. Su, Z.-Y. Zhou, Y.-G. Zheng, H. Sun, B. Yang, P. Hauke, W. Zheng, J. C. Halimeh, Z.-S. Yuan, and J.-W. Pan, Observation of microscopic confinement dynamics by a tunable topological θ-angle, Nat. Phys. **21**, 155 (2025).

[11] R. C. Farrell, M. Illa, A. N. Ciavarella, and M. J. Savage, Scalable circuits for preparing ground states on digital quantum computers: The Schwinger model vacuum on 100 qubits, PRX Quantum **5**, 020315 (2024).

[12] J. Knaute, Meson content of entanglement spectra after integrable and nonintegrable quantum quenches, Phys. Rev. B **107**, L100303 (2023).

[13] H.-Y. Qi and W. Zheng, Gauge violation spectroscopy of synthetic gauge theories, Phys. Rev. Res. **6**, 013047 (2024).

[14] Z. Davoudi, N. Mueller, and C. Powers, Towards quantum computing phase diagrams of gauge theories with thermal pure quantum states, Phys. Rev. Lett. **131**, 081901 (2023).

[15] M. Fromm, O. Philipsen, M. Spannowsky, and C. Winterowd, Simulating Z_2 lattice gauge theory with the variational quantum thermalizer, EPJ Quantum Technol. **11**, 20 (2024).

[16] M. Kebrič, J. C. Halimeh, U. Schollwöck, and F. Grusdt, Confinement in $(1+1)$-dimensional z_2 lattice gauge theories at finite temperature, Phys. Rev. B **109**, 245110 (2024).

[17] M. Kormos, M. Collura, G. Takács, and P. Calabrese, Real-time confinement following a quantum quench to a non-integrable model, Nat. Phys. **13**, 246 (2017).

[18] F. Liu, R. Lundgren, P. Titum, G. Pagano, J. Zhang, C. Monroe, and A. V. Gorshkov, Confined quasiparticle dynamics in long-range interacting quantum spin chains, Phys. Rev. Lett. **122**, 150601 (2019).

[19] J. C. Halimeh, M. Van Damme, V. Zauner-Stauber, and L. Vanderstraeten, Quasiparticle origin of dynamical quantum phase transitions, Phys. Rev. Res. **2**, 033111 (2020).

[20] N. Ranabhat, A. Santini, E. Tirrito, and M. Collura, Dynamical deconfinement transition driven by density of excitations, Phys. Rev. B **111**, 024304 (2025).

[21] A. A. Belavin, A. M. Polyakov, and A. B. Zamolodchikov, Infinite conformal symmetry of critical fluctuations in two dimensions, J. Stat. Phys. **34**, 763 (1984).

[22] M. Henkel and H. Saleur, The two-dimensional Ising model in the magnetic field: A numerical check of Zamolodchikov's conjecture, J. Phys. A: Math. Gen. **22**, L513 (1989).

[23] R. D. Sedgewick, D. J. Scalapino, and R. L. Sugar, Fractionalized phase in an XY $- Z_2$ gauge model, Phys. Rev. B **65**, 054508 (2002).

[24] T. Pichler, M. Dalmonte, E. Rico, P. Zoller, and S. Montangero, Real-time dynamics in U(1) lattice gauge theories with tensor networks, Phys. Rev. X **6**, 011023 (2016).

[25] B. Neyenhuis, J. Zhang, P. W. Hess, J. Smith, A. C. Lee, P. Richerme, Z.-X. Gong, A. V. Gorshkov, and C. Monroe, Observation of prethermalization in long-range interacting spin chains, Sci. Adv. **3**, e1700672 (2017).

[26] J. C. P. Barros, M. Dalmonte, and A. Trombettoni, String tension and robustness of confinement properties in the Schwinger-Thirring model, Phys. Rev. D **100**, 036009 (2019).

[27] G. Magnifico, M. Dalmonte, P. Facchi, S. Pascazio, F. V. Pepe, and E. Ercolessi, Real time dynamics and confinement in the $\mathbb{Z}_n$ Schwinger-Weyl lattice model for 1+1 QED, Quantum **4**, 281 (2020).

[28] A. Lerose, B. Žunkovič, A. Silva, and A. Gambassi, Quasilocalized excitations induced by long-range interactions in

translationally invariant quantum spin chains, Phys. Rev. B **99**, 121112 (2019).

[29] W. L. Tan, P. Becker, F. Liu, G. Pagano, K. S. Collins, A. De, L. Feng, H. B. Kaplan, A. Kyprianidis, R. Lundgren, W. Morong, S. Whitsitt, A. V. Gorshkov, and C. Monroe, Domain-wall confinement and dynamics in a quantum simulator, Nat. Phys. **17**, 742 (2021).

[30] J. Vovrosh and J. Knolle, Confinement and entanglement dynamics on a digital quantum computer, Sci. Rep. **11**, 11577 (2021).

[31] G. Lagnese, F. M. Surace, M. Kormos, and P. Calabrese, False vacuum decay in quantum spin chains, Phys. Rev. B **104**, L201106 (2021).

[32] A. Silva, Statistics of the work done on a quantum critical system by quenching a control parameter, Phys. Rev. Lett. **101**, 120603 (2008).

[33] M. Heyl, A. Polkovnikov, and S. Kehrein, Dynamical quantum phase transitions in the transverse-field Ising model, Phys. Rev. Lett. **110**, 135704 (2013).

[34] M. Heyl, Dynamical quantum phase transitions: A review, Rep. Prog. Phys. **81**, 054001 (2018).

[35] C. Karrasch and D. Schuricht, Dynamical phase transitions after quenches in nonintegrable models, Phys. Rev. B **87**, 195104 (2013).

[36] S. Vajna and B. Dóra, Disentangling dynamical phase transitions from equilibrium phase transitions, Phys. Rev. B **89**, 161105 (2014).

[37] F. Andraschko and J. Sirker, Dynamical quantum phase transitions and the Loschmidt echo: A transfer matrix approach, Phys. Rev. B **89**, 125120 (2014).

[38] B. Žunkovič, A. Silva, and M. Fabrizio, Dynamical phase transitions and Loschmidt echo in the infinite-range XY model, Philos. Trans. R. Soc. A **374**, 20150160 (2016).

[39] J. C. Halimeh and V. Zauner-Stauber, Dynamical phase diagram of quantum spin chains with long-range interactions, Phys. Rev. B **96**, 134427 (2017).

[40] V. Zauner-Stauber and J. C. Halimeh, Probing the anomalous dynamical phase in long-range quantum spin chains through Fisher-zero lines, Phys. Rev. E **96**, 062118 (2017).

[41] I. Homrighausen, N. O. Abeling, V. Zauner-Stauber, and J. C. Halimeh, Anomalous dynamical phase in quantum spin chains with long-range interactions, Phys. Rev. B **96**, 104436 (2017).

[42] B. Žunkovič, M. Heyl, M. Knap, and A. Silva, Dynamical quantum phase transitions in spin chains with long-range interactions: Merging different concepts of nonequilibrium criticality, Phys. Rev. Lett. **120**, 130601 (2018).

[43] N. Defenu, T. Enss, and J. C. Halimeh, Dynamical criticality and domain-wall coupling in long-range Hamiltonians, Phys. Rev. B **100**, 014434 (2019).

[44] P. Uhrich, N. Defenu, R. Jafari, and J. C. Halimeh, Out-of-equilibrium phase diagram of long-range superconductors, Phys. Rev. B **101**, 245148 (2020).

[45] J. C. Halimeh, M. Van Damme, L. Guo, J. Lang, and P. Hauke, Dynamical phase transitions in quantum spin models with antiferromagnetic long-range interactions, Phys. Rev. B **104**, 115133 (2021).

[46] A. L. Corps and A. Relaño, Dynamical and excited-state quantum phase transitions in collective systems, Phys. Rev. B **106**, 024311 (2022).

[47] A. L. Corps and A. Relaño, Theory of dynamical phase transitions in quantum systems with symmetry-breaking eigenstates, Phys. Rev. Lett. **130**, 100402 (2023).

[48] A. Mitra, T. Albash, P. D. Blocher, J. Takahashi, A. Miyake, G. Biedermann, and I. H. Deutsch, Macroproperties vs microstates in the classical simulation of critical phenomena in quench dynamics of 1D Ising models, New J. Phys. **27**, 013026 (2025).

[49] S. Vajna and B. Dóra, Topological classification of dynamical phase transitions, Phys. Rev. B **91**, 155127 (2015).

[50] M. Schmitt and S. Kehrein, Dynamical quantum phase transitions in the Kitaev honeycomb model, Phys. Rev. B **92**, 075114 (2015).

[51] N. Sedlmayr, P. Jaeger, M. Maiti, and J. Sirker, Bulk-boundary correspondence for dynamical phase transitions in one-dimensional topological insulators and superconductors, Phys. Rev. B **97**, 064304 (2018).

[52] I. Hagymási, C. Hubig, O. Legeza, and U. Schollwöck, Dynamical topological quantum phase transitions in nonintegrable models, Phys. Rev. Lett. **122**, 250601 (2019).

[53] T. Masłowski and N. Sedlmayr, Quasiperiodic dynamical quantum phase transitions in multiband topological insulators and connections with entanglement entropy and fidelity susceptibility, Phys. Rev. B **101**, 014301 (2020).

[54] S. Porta, F. Cavaliere, M. Sassetti, and N. T. Ziani, Topological classification of dynamical quantum phase transitions in the xy chain, Sci. Rep. **10**, 12766 (2020).

[55] R. Okugawa, H. Oshiyama, and M. Ohzeki, Mirror-symmetry-protected dynamical quantum phase transitions in topological crystalline insulators, Phys. Rev. Res. **3**, 043064 (2021).

[56] K. Wrześniewski, I. Weymann, N. Sedlmayr, and T. Domański, Dynamical quantum phase transitions in a mesoscopic superconducting system, Phys. Rev. B **105**, 094514 (2022).

[57] T. Masłowski and N. Sedlmayr, Dynamical bulk-boundary correspondence and dynamical quantum phase transitions in higher-order topological insulators, Phys. Rev. B **108**, 094306 (2023).

[58] U. Bhattacharya and A. Dutta, Emergent topology and dynamical quantum phase transitions in two-dimensional closed quantum systems, Phys. Rev. B **96**, 014302 (2017).

[59] S. A. Weidinger, M. Heyl, A. Silva, and M. Knap, Dynamical quantum phase transitions in systems with continuous symmetry breaking, Phys. Rev. B **96**, 134313 (2017).

[60] M. Heyl, F. Pollmann, and B. Dóra, Detecting equilibrium and dynamical quantum phase transitions in Ising chains via out-of-time-ordered correlators, Phys. Rev. Lett. **121**, 016801 (2018).

[61] S. D. Nicola, B. Doyon, and M. J. Bhaseen, Stochastic approach to non-equilibrium quantum spin systems, J. Phys. A: Math. Theor. **52**, 05LT02 (2019).

[62] T. Hashizume, J. C. Halimeh, and I. P. McCulloch, Hybrid infinite time-evolving block decimation algorithm for long-range multidimensional quantum many-body systems, Phys. Rev. B **102**, 035115 (2020).

[63] T. Hashizume, J. C. Halimeh, P. Hauke, and D. Banerjee, Ground-state phase diagram of quantum link electrodynamics in $(2+1)$-d, SciPost Phys. **13**, 017 (2022).

[64] N. O. Abeling and S. Kehrein, Quantum quench dynamics in the transverse field Ising model at nonzero temperatures, Phys. Rev. B **93**, 104302 (2016).

[65] U. Bhattacharya, S. Bandyopadhyay, and A. Dutta, Mixed state dynamical quantum phase transitions, Phys. Rev. B **96**, 180303 (2017).

[66] M. Heyl and J. C. Budich, Dynamical topological quantum phase transitions for mixed states, Phys. Rev. B **96**, 180304 (2017).

[67] N. Sedlmayr, M. Fleischhauer, and J. Sirker, Fate of dynamical phase transitions at finite temperatures and in open systems, Phys. Rev. B **97**, 045147 (2018).

[68] J. Lang, B. Frank, and J. C. Halimeh, Concurrence of dynamical phase transitions at finite temperature in the fully connected transverse-field Ising model, Phys. Rev. B **97**, 174401 (2018).

[69] J. Lang, B. Frank, and J. C. Halimeh, Dynamical quantum phase transitions: A geometric picture, Phys. Rev. Lett. **121**, 130603 (2018).

[70] T. V. Zache, N. Mueller, J. T. Schneider, F. Jendrzejewski, J. Berges, and P. Hauke, Dynamical topological transitions in the massive Schwinger model with a θ term, Phys. Rev. Lett. **122**, 050403 (2019).

[71] Y.-P. Huang, D. Banerjee, and M. Heyl, Dynamical quantum phase transitions in $U(1)$ quantum link models, Phys. Rev. Lett. **122**, 250401 (2019).

[72] S. P. Pedersen and N. T. Zinner, Lattice gauge theory and dynamical quantum phase transitions using noisy intermediate-scale quantum devices, Phys. Rev. B **103**, 235103 (2021).

[73] R. B. Jensen, S. P. Pedersen, and N. T. Zinner, Dynamical quantum phase transitions in a noisy lattice gauge theory, Phys. Rev. B **105**, 224309 (2022).

[74] M. Van Damme, T. V. Zache, D. Banerjee, P. Hauke, and J. C. Halimeh, Dynamical quantum phase transitions in spin-$SU(1)$ quantum link models, Phys. Rev. B **106**, 245110 (2022).

[75] N. Mueller, J. A. Carolan, A. Connelly, Z. Davoudi, E. F. Dumitrescu, and K. Yeter-Aydeniz, Quantum computation of dynamical quantum phase transitions and entanglement tomography in a lattice gauge theory, PRX Quantum **4**, 030323 (2023).

[76] D. Pomarico, L. Cosmai, P. Facchi, C. Lupo, S. Pascazio, and F. V. Pepe, Dynamical quantum phase transitions of the Schwinger model: Real-time dynamics on IBM quantum, Entropy **25**, 608 (2023).

[77] P. Jurcevic, H. Shen, P. Hauke, C. Maier, T. Brydges, C. Hempel, B. P. Lanyon, M. Heyl, R. Blatt, and C. F. Roos, Direct observation of dynamical quantum phase transitions in an interacting many-body system, Phys. Rev. Lett. **119**, 080501 (2017).

[78] N. Fläschner, D. Vogel, M. Tarnowski, B. S. Rem, D.-S. Lühmann, M. Heyl, J. C. Budich, L. Mathey, K. Sengstock, and C. Weitenberg, Observation of dynamical vortices after quenches in a system with topology, Nat. Phys. **14**, 265 (2018).

[79] X. Nie, B.-B. Wei, X. Chen, Z. Zhang, X. Zhao, C. Qiu, Y. Tian, Y. Ji, T. Xin, D. Lu, and J. Li, Experimental observation of equilibrium and dynamical quantum phase transitions via out-of-time-ordered correlators, Phys. Rev. Lett. **124**, 250601 (2020).

[80] D. J. Thouless, Long-range order in one-dimensional Ising systems, Phys. Rev. **187**, 732 (1969).

[81] V. L. Berezinskii, Destruction of long-range order in one-dimensional and two-dimensional systems having a continuous symmetry group I. Classical systems, J. Exp. Theor. Phys. **32**, 493 (1971).

[82] J. M. Kosterlitz, Phase transitions in long-range ferromagnetic chains, Phys. Rev. Lett. **37**, 1577 (1976).

[83] A. Dutta and J. K. Bhattacharjee, Phase transitions in the quantum Ising and rotor models with a long-range interaction, Phys. Rev. B **64**, 184106 (2001).

[84] S. Sachdev, *Quantum Phase Transitions* (Cambridge University Press, Cambridge, 1999).

[85] I. P. McCulloch, Infinite size density matrix renormalization group, revisited, arXiv:0804.2509.

[86] U. Schollwöck, The density-matrix renormalization group in the age of matrix product states, Ann. Phys. (NY) **326**, 96 (2011).

[87] S. Paeckel, T. Köhler, A. Swoboda, S. R. Manmana, U. Schollwöck, and C. Hubig, Time-evolution methods for matrix-product states, Ann. Phys. (NY) **411**, 167998 (2019).

[88] I. P. McCulloch and J. J. Osborne, Matrix product toolkit, https://github.com/mptoolkit.

[89] J. Haegeman, J. I. Cirac, T. J. Osborne, I. Pižorn, H. Verschelde, and F. Verstraete, Time-dependent variational principle for quantum lattices, Phys. Rev. Lett. **107**, 070601 (2011).

[90] J. Haegeman, C. Lubich, I. Oseledets, B. Vandereycken, and F. Verstraete, Unifying time evolution and optimization with matrix product states, Phys. Rev. B **94**, 165116 (2016).

[91] G. M. Crosswhite, A. C. Doherty, and G. Vidal, Applying matrix product operators to model systems with long-range interactions, Phys. Rev. B **78**, 035116 (2008).

[92] V. Zauner, D. Draxler, L. Vanderstraeten, M. Degroote, J. Haegeman, M. M. Rams, V. Stojevic, N. Schuch, and F. Verstraete, Transfer matrices and excitations with matrix product states, New J. Phys. **17**, 053002 (2015).

[93] B. Sciolla and G. Biroli, Quantum quenches and off-equilibrium dynamical transition in the infinite-dimensional Bose-Hubbard model, Phys. Rev. Lett. **105**, 220401 (2010).

[94] B. Sciolla and G. Biroli, Dynamical transitions and quantum quenches in mean-field models, J. Stat. Mech. (2011) P11003.

[95] L. Vanderstraeten, M. Van Damme, H. P. Büchler, and F. Verstraete, Quasiparticles in quantum spin chains with long-range interactions, Phys. Rev. Lett. **121**, 090603 (2018).

[96] J. Haegeman, B. Pirvu, D. J. Weir, J. I. Cirac, T. J. Osborne, H. Verschelde, and F. Verstraete, Variational matrix product ansatz for dispersion relations, Phys. Rev. B **85**, 100408 (2012).

[97] J. J. Osborne and I. P. McCulloch, Efficient and systematic calculation of arbitrary observables for the matrix product state excitation ansatz, Phys. Rev. Res. **7**, 023018 (2025).

[98] L. Onsager, Crystal statistics. I. A two-dimensional model with an order-disorder transition, Phys. Rev. **65**, 117 (1944).

[99] M. S. L. du Croo de Jongh and J. M. J. van Leeuwen, Critical behavior of the two-dimensional Ising model in a transverse field: A density-matrix renormalization calculation, Phys. Rev. B **57**, 8494 (1998).

[100] H. W. J. Blöte and Y. Deng, Cluster Monte Carlo simulation of the transverse Ising model, Phys. Rev. E **66**, 066110 (2002).

[101] T. Hashizume, I. P. McCulloch, and J. C. Halimeh, Dynamical phase transitions in the two-dimensional transverse-field Ising model, Phys. Rev. Res. **4**, 013250 (2022).

[102] S. Chandrasekharan and U.-J. Wiese, Quantum link models: A discrete approach to gauge theories, Nucl. Phys. B **492**, 455 (1997).

[103] U.-J. Wiese, Ultracold quantum gases and lattice systems: Quantum simulation of lattice gauge theories, Ann. Phys. (NY) **525**, 777 (2013).

[104] V. Kasper, F. Hebenstreit, F. Jendrzejewski, M. K. Oberthaler, and J. Berges, Implementing quantum electrodynamics with ultracold atomic systems, New J. Phys. **19**, 023030 (2017).

[105] S. Coleman, More about the massive Schwinger model, Ann. Phys. (NY) **101**, 239 (1976).

[106] E. Rico, T. Pichler, M. Dalmonte, P. Zoller, and S. Montangero, Tensor networks for lattice gauge theories and atomic quantum simulation, Phys. Rev. Lett. **112**, 201601 (2014).

[107] G.-X. Su, H. Sun, A. Hudomal, J.-Y. Desaules, Z.-Y. Zhou, B. Yang, J. C. Halimeh, Z.-S. Yuan, Z. Papić, and J.-W. Pan, Observation of many-body scarring in a Bose-Hubbard quantum simulator, Phys. Rev. Res. **5**, 023010 (2023).

[108] J. Osborne, B. Yang, I. P. McCulloch, P. Hauke, and J. C. Halimeh, Spin-S U(1) quantum link models with dynamical matter on a quantum simulator, arXiv:2305.06368.